

Photoconductivity of functionalized carbon nanotubes

R. G. Abaszade^{a,b,*}, A. G. Mammadov^a, E. A. Khanmamedova^a, F. G. Aliyev^b,
V. O. Kotsyubynsky^c, E. Gür^d, B. D. Soltabayev^e, T.O. Margitych^f,
M. O. Stetsenko^{g,h}, A. Singhⁱ, S. Aryaⁱ

^aAzerbaijan State Oil and Industry University, Baku, Azerbaijan,

^bAzerbaijan University of Architecture and Construction, Baku, Azerbaijan,

^cVasyl Stefanyk Precarpathian National University, Ivano-Frankivsk, Kyiv, Ukraine,

^dEskisehir Osmangazi University, Eskisehir 26040, Turkey

^eNazarbayev University, Nur-Sultan 010000, Astana, Kazakhstan

^fKyiv Institute for Nuclear Research, National Academy of Sciences of Ukraine, 03680, Kyiv, Ukraine

^gKey Laboratory of Optoelectronic Devices and Systems of Ministry of Education and Guangdong Province, College of Physics and Optoelectronic Engineering, Shenzhen University, 518060, Shenzhen, PR China

^hV.E. Lashkarev Institute of Semiconductor Physics, National Academy of Science of Ukraine, Kyiv, Ukraine,

ⁱDepartment of Physics, University of Jammu, Jammu 180006, India

Investigation of carbon nanotubes is a modern trend due to their combination of unique physical, chemical, electrical, and optical properties. Carboxyl-functionalized carbon nanotubes (fCNTs) for investigation of photoelectrical properties were synthesized. The photo-sensitivity spectra of a carboxyl-functionalized CNT sample for voltage range from 1 to 9 V, and for the spectral range from 400 to 900 nm were investigated. The voltage equal to 1 V generated lower photosensitivity in the broadband wavelength range for visible to near-infrared. The most efficient photocurrents of fCNTs were received for a voltage of 5 V in the wavelength range $\lambda_p \sim 400\text{--}800$ nm and for voltage $U=3\text{V}$ in the broadband spectral range $\lambda_p \sim 400\text{--}900$ nm. The experimental data analysis helped to determine the widest photosensitivity range, as well as the highest sensitivity value. As result, the voltage $U=5\text{V}$ was obtained. Here, the most significant photocurrent peak with $I_p \sim 2.67 \mu\text{A}$ for wavelength $\lambda \sim 720$ nm was observed. A comparison between the photosensitivity spectra of fCNTs and pure CNTs shows that the photosensitivity of fCNTs has increased significantly. Thus, the maximum photosensitivity for fCNTs is $I_p \sim 2.67 \mu\text{A}$, and for pure CNTs, it equals $I_p \sim 0.185 \mu\text{A}$. A 14-fold enhancement of photosensitivity for fCNT has been registered. The mathematical analysis of spectral dependencies of generated photocurrents under different applied voltages can be described using fourth-order polynomials. The I-V characteristics for wavelengths 760 nm and 780 nm have the same trend with the shift of photocurrent maximum to the lower parameters of voltage. The carboxyl-functionalized nanotubes can be effectively used as light detectors and in optoelectronic applications.

(Received February 20, 2024; Accepted June 7, 2024)

Keywords: Functionalized carbon nanotubes, Photocurrent, Photosensitivity

1. Introduction

A lot of optoelectronic applications are working using carbon low-dimensional nanomaterials (carbon nanotubes, graphene, and its derivatives). Modern investigation of carbon nanocomposite connected with optical, photoelectrical, and structural properties characterization for new applications [1-8]. The most useful synthesis methods for carbon nanotubes are the arc

* Corresponding author: abaszada@gmail.com

<https://doi.org/10.15251/DJNB.2024.192.837>

discharge method, laser ablation method, and chemical vapor deposition method [9]. Surface functionalization of carbon nanomaterials and nanocomposites can be processed by different strategies [9]: non-covalent binding [10-11] and covalent binding [12-13], nanoparticle functionalization [14-16,30]. A new fullerene-activated carbon nanotube detector with high photosensitivity has been proposed [17]. Electrochemical biosensors based on carbon are perspective medical applications and bioimaging techniques [18]. The electrical properties and photoelectrical phenomena for carbon and composite nanomaterials are explained in [19-23]. In [24-29] physical properties of CNTs and GO were comparatively investigated. In the paper [24], the morphology and structural parameters of carbon nanotubes and gadolinium-doped carbon nanotubes were investigated by using Scanning Electron Microscopy and X-ray diffraction techniques. Optical and structural properties of carbon nanotubes doped with 10% and 15% gadolinium were shown in [24-26]. Doping degree transformed the physical and chemical properties of carbon nanotubes. In our previous research [27], the photosensitivity spectral characteristics for pure CNTs in the wavelengths from 400 up to 900 nm at different applied voltages to the sample were studied and received new information for the next generation of photoelectrical and optoelectronic CNTs devices.

2. Experimental details

Carbon nanotubes were obtained by the arc discharge method and initially functionalized with a carboxyl group. For the measurement of photoelectrical properties, the home-built setup consisting of a white light source, monochromator, and digital registration electronics was used at room temperature [27].

3. Results

Spectral characteristics of carbon nanotube functionalized with the carboxyl group photosensitivity under different wavelengths (400-900 nm) of excitation light at two applied voltage values 1V and 3V are described in Figure 1. The spectral dependencies of photocurrent (Figure 1) indicate that for the spectral range, $\lambda=600$ -875 nm with maxima at $\lambda_{p1}\sim 600$ nm, $\lambda_{p2}\sim 700$ nm, $\lambda_{p3}\sim 760$ nm, $\lambda_{p4}\sim 840$ nm, $\lambda_{p5}\sim 875$ nm the photocurrent intensities for $U=1$ V were evenly distributed.

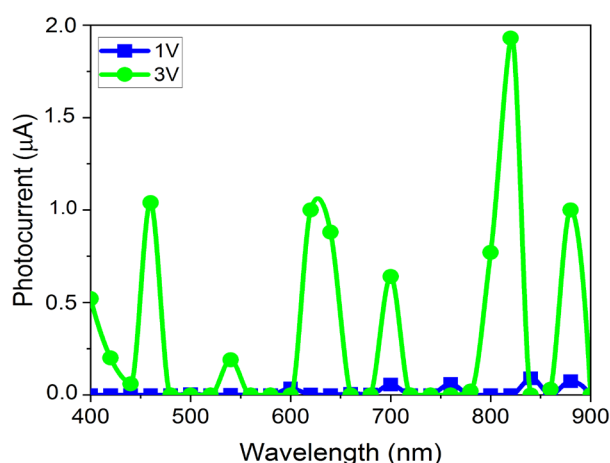


Fig. 1. Photosensitivity spectra of carboxyl functionalized carbon nanotubes for applied voltages $U=1V$ and $U=3V$.

The highest amplitude of photosensitivity equal to $0.1 \mu\text{A}$ is registered at $\lambda_{p4} \sim 840 \text{ nm}$. Other peaks have a photocurrent value less than $0.1 \mu\text{A}$. In the spectral range from 400 to 575 nm, the absence (zero) of photosensitivity is observed. Almost the entire investigated spectral range $\lambda = 400\text{--}900 \text{ nm}$ at $U = 1\text{V}$ is characterized as small intensity light sensitivity range. Photocurrent intensity peaks with the wavelengths $\lambda_{p1} \sim 400 \text{ nm}$, $\lambda_{p2} \sim 460 \text{ nm}$, $\lambda_{p3} \sim 540 \text{ nm}$, $\lambda_{p4} \sim 620 \text{ nm}$, $\lambda_{p5} \sim 700 \text{ nm}$, $\lambda_{p6} \sim 820 \text{ nm}$, $\lambda_{p7} \sim 875 \text{ nm}$ at voltage value $U = 3 \text{ V}$ are observed. In comparison with the photocurrent for $\lambda_{p6} \sim 820 \text{ nm}$ at $U = 1\text{V}$ the photocurrent for $U = 3\text{V}$ has a maximum peak with a significant increase up to $I_{p6} \sim 1.93 \mu\text{A}$. The spectral peak position $\lambda_{p6} \sim 820 \text{ nm}$ is slightly shifted to the low wavelength spectral range. Zero photosensitivity in the spectral range $\lambda = 475\text{--}525 \text{ nm}$ was detected. In this case, the range of zero photosensitivity has narrowed.

Figure 2 shows the spectral characteristics of photosensitivity for fCNT in the spectral range from UV to NIR at three values of the bias voltage U (5 V, 7 V, and 9 V) applied to the investigated sample.

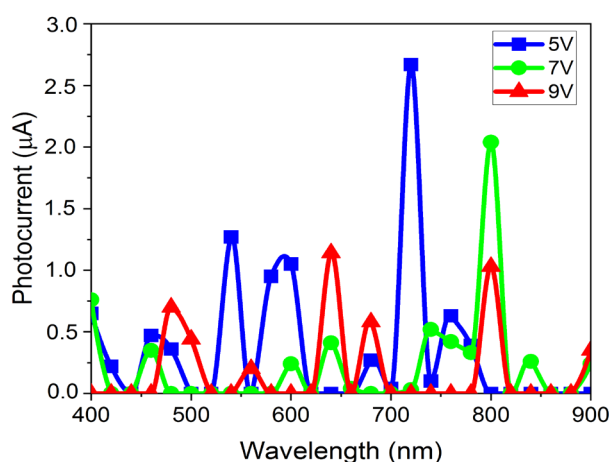


Fig. 2. The photosensitivity spectral dependencies of fCNTs for the bias voltages U (5V, 7V, and 9V) applied to the sample.

At $U = 5 \text{ V}$, the peaks for wavelengths $\lambda_{p1} \sim 400 \text{ nm}$, $\lambda_{p2} \sim 460 \text{ nm}$, $\lambda_{p3} \sim 540 \text{ nm}$, $\lambda_{p4} \sim 600 \text{ nm}$, $\lambda_{p5} \sim 675 \text{ nm}$, $\lambda_{p6} \sim 720 \text{ nm}$, $\lambda_{p7} \sim 760 \text{ nm}$ are registered. The maximum peak at wavelength $\lambda_{p6} \sim 720 \text{ nm}$ with photocurrent value $I_{p6} \sim 2.67 \mu\text{A}$ is observed. The third peak at $\lambda_{p3} \sim 540 \text{ nm}$ and the fourth peak at $\lambda_{p4} \sim 600 \text{ nm}$ have photocurrent values $I_{p3} \sim 1.27 \mu\text{A}$ and $I_{p4} \sim 1.05 \mu\text{A}$, respectively. The zero photosensitivity spectral range $\lambda = 800\text{--}900 \text{ nm}$ is $\Delta\lambda = 100 \text{ nm}$. At voltage $U = 7 \text{ V}$, the maximum intensities of photocurrent for wavelengths $\lambda_{p1} \sim 400 \text{ nm}$, $\lambda_{p2} \sim 460 \text{ nm}$, $\lambda_{p3} \sim 600 \text{ nm}$, $\lambda_{p4} \sim 635 \text{ nm}$, $\lambda_{p5} \sim 740 \text{ nm}$, $\lambda_{p6} \sim 800 \text{ nm}$, and $\lambda_{p7} \sim 840 \text{ nm}$ were registered. The maximum peak at wavelength $\lambda_{p6} \sim 800 \text{ nm}$ with photocurrent value $I_{p6} \sim 2.04 \mu\text{A}$ was observed. Other peaks have a small photocurrent value of less than $0.5 \mu\text{A}$. At the spectral range, $\lambda = 475\text{--}575 \text{ nm}$ with zero photosensitivity was registered. At voltage $U = 9\text{V}$, for spectral range $\lambda = 520\text{--}620 \text{ nm}$ ($\Delta\lambda = 100 \text{ nm}$) the weak photosensitivity spectra were registered. This spectral range has one weak photocurrent peak at wavelength $\lambda_{p2} \sim 560 \text{ nm}$. The maxima values of photocurrent $I_{p3} \sim 1.14 \mu\text{A}$ and $I_{p5} \sim 1.03 \mu\text{A}$ were observed at wavelength $\lambda_{p3} \sim 640 \text{ nm}$ and $\lambda_{p5} \sim 800 \text{ nm}$, respectively. The peaks at wavelengths $\lambda_{p1} \sim 475 \text{ nm}$ and $\lambda_{p4} \sim 680 \text{ nm}$ correspond to photocurrent values $I_{p1} \sim 0.7 \mu\text{A}$ and $I_{p4} \sim 0.58 \mu\text{A}$, respectively.

The analysis of measured photocurrent spectra shows that the increase in applied voltage (up to 9V) to the investigated fCNT sample leads to an increase in photosensitivity. The photocurrent data at voltage $U = 1\text{V}$ for spectral range $\lambda = 400\text{--}900 \text{ nm}$ with small photosensitivity characterized it as ineffective for light detection. The most efficient use of fCNT is on the voltage 5 V in the wavelength range $\lambda_p \sim 400\text{--}800 \text{ nm}$ and voltage $U = 3\text{V}$ in the wavelength range $\lambda_p \sim 400\text{--}900 \text{ nm}$. For widest spectral range and the highest photosensitivity values can be used at the voltage value $U = 5 \text{ V}$. Figure 2 shows, the photocurrent at the wavelength $\lambda \sim 720 \text{ nm}$ reaches a

value equal to $I_p \sim 2.67 \mu\text{A}$. These experimental results indicate that fCNTs can be effectively used as light detectors in the tuned wavelength range. A comparison between the photosensitivity spectra of fCNTs and pure CNTs [27] shows that the photosensitivity for fCNTs has increased significantly. Thus, the maximum photosensitivity for carbon nanotubes functionalized with a carboxyl group and for pure carbon nanotubes equals $I_p \sim 2.67 \mu\text{A}$ and $I_p \sim 0.185 \mu\text{A}$, relatively. A 14-fold enhancement of light sensitivity for fCNTs has been observed. The photosensitivity experimental spectral dependencies at different voltage values can be transformed into I-V characteristics for understanding photoelectrical features of light interaction with fCNTs.

It is of interest to study the observed changes in the photosensitivity ranges for fCNTs as well as their intensities after changing the voltage applied to the samples. It is from this point of view that we draw the graph of the dependence of the voltages on the photosensitivity spectrum at different wavelengths. As can be seen from the figure, the I-V characteristics of the samples used for different wavelengths are described as follows. The I-V characteristics fCNTs (Figure 3(a)) for wavelengths 640 nm and 720 nm can be approximated using the next approach:

$$I = -0.01047 \cdot U^4 + 0.231 \cdot U^3 - 1.692 \cdot U^2 + 4.624 \cdot U - 3.152 \quad (1)$$

$$I = 0.04141 \cdot U^4 - 0.8288 \cdot U^3 + 5.391 \cdot U^2 - 12.45 \cdot U + 7.843 \quad (1)$$

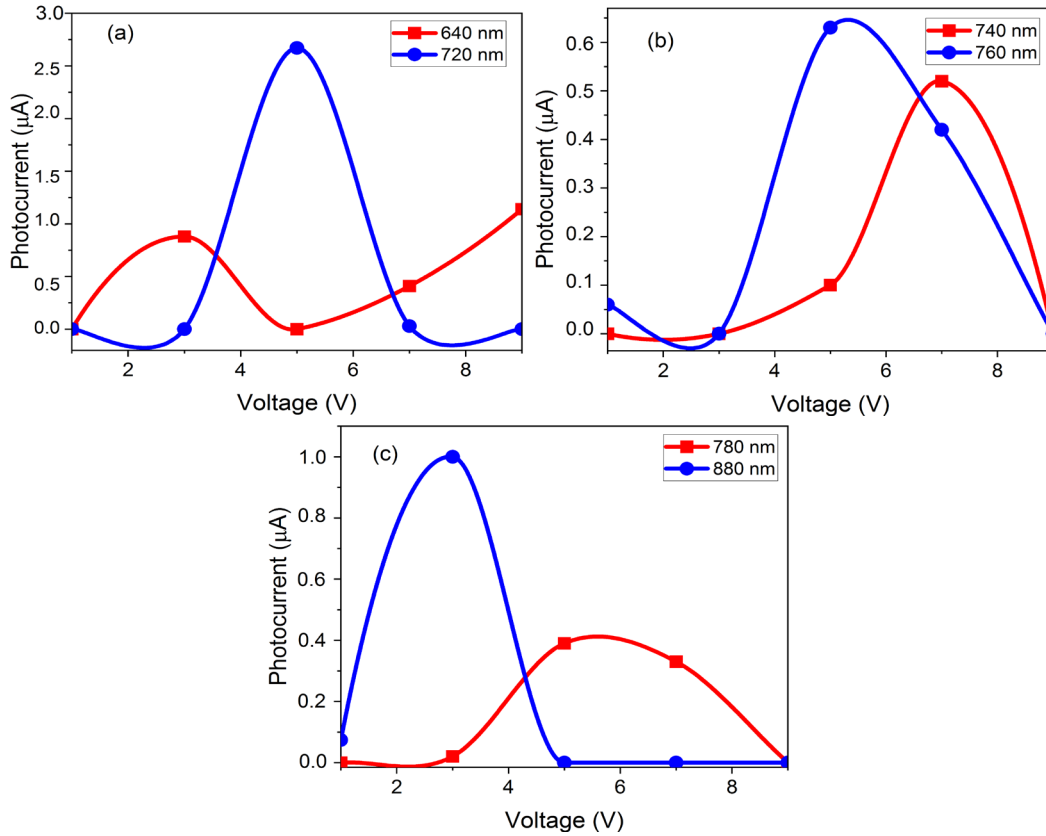


Fig. 3. I-V curves of fCNT for different illumination wavelengths.

I-V characteristics as shown in Figure 3 included different regions that can be associated with specific conductance for carbon materials. The voltage ranges 2.2-5V at wavelength $\lambda \sim 640$ nm and in the ranges 1-2.1 V and 6-8.7 V can indicate the presence of negative differential conductance (Figure 3 (a)). Also, another region can be associated with appearing of positive differential conductivity. From the I-V curve at the wavelength 720 nm (Figure 3 (a)), the voltage ranges of 1-3 V and 7-9 V can be associated with zero sensitivity area. In addition, the voltage range 5-7V can be described with an influence of the negative differential photoconductivity

mechanism. The voltage $U=5V$ and illumination wavelength 720 nm lead to the generation of a maximum photocurrent value equal to $I_p \sim 2.7 \mu A$. The absorbed light generated the electron-hole pair's formation. This process (separation of electron-hole pairs) can be controlled by the bias voltage. The carrier concentration will be increased as well as the conductivity and current. I-V characteristics in Figure 3(b) at two wavelengths 740 nm and 760 nm can be approximated by:

$$I = -0.003854 \cdot U^4 + 0.06625 \cdot U^3 - 0.3602 \cdot U^2 + 0.7338 \cdot U - 0.4359 \quad (3)$$

$$I = 0.005625 \cdot U^4 - 0.1219 \cdot U^3 + 0.8569 \cdot U^2 - 2.098 \cdot U + 1.418 \quad (4)$$

I-V curve in Figure 3(b) for wavelength $\lambda \sim 740$ nm and the voltage ranges 1-1.5 V and 4.2-7.5 V can be associated with appearing of positive differential photoconductivity. Other voltage ranges 1.7-3 V and 7.5-9 V can be associated with a negative differential photoconductivity mechanism. The voltage 3-4.2V range indicated the presence of an almost zero photosensitivity. The maximum photocurrent value equal to $I_p \sim 0.55 \mu A$ is reached at $U=7.5V$. The weak photosensitivity intensity with a photocurrent value equal to $I_p \sim 0.06 \mu A$ takes place at $U=1.6V$. Thus, the maximum photocurrent value decreased and shifted towards higher voltage values with an increase of wavelength from 740 to 760 nm. From I-V curve in Figure 3(b) at wavelength $\lambda \sim 760$ nm also can be associated with two different mechanisms of photoconductivity. The features of the I-V curve for voltage range 5.5-8.5V and 3-5.5V can be connected with negative and positive differential photoconductivity, respectively. In this case, zero sensitivity region was registered in the two voltage ranges 1-3 V and 8.5-9 V. The voltage $U=5.5V$ generated the maximum photocurrent value equal to $I_p \sim 0.67 \mu A$, and the peak position shifted towards lower voltage values. Figure 3(c) shows the experimental data of I-V curves of fCNT for two wavelengths, $\lambda \sim 780$ nm, and $\lambda \sim 880$ nm. For these curves, the following fitting approach has been applied:

$$I = 0.002448 \cdot U^4 - 0.05542 \cdot U^3 + 0.4005 \cdot U^2 - 0.9696 \cdot U + 0.622 \quad (5)$$

$$I = -0.01022 \cdot U^4 + 0.2245 \cdot U^3 - 1.669 \cdot U^2 + 4.627 \cdot U - 3.099 \quad (6)$$

4. Discussion

I-V curves at the wavelengths 780 nm have the same shape as the wavelength 760 nm. The maximum value of photocurrent was maintained at the voltage value $U=5.5V$ but slightly decreased up to the value $0.42 \mu A$. The voltage range with zero light sensitivity takes place from 1 to 3 V under 780 nm illumination light. For illumination with wavelength 880 nm, zero light sensitivity area in the range from 5 to 9V, was detected. The photocurrent peaks with values $1.1 \mu A$ and $1.2 \mu A$ are registered at $U=2.2V$ and $U=9V$, respectively. The voltage ranges of 2.3-5V and 8.2-9V at illumination 880 nm on the I-V curve (Figure 3 (c)) can be associated with negative differential photoconductivity. The region of zero light sensitivity from voltage 5 to 7 V was registered. A weak peak at voltage $U=8.2V$ with a photocurrent value of $0.24 \mu A$ was detected. The photocurrent peak intensity shifted towards lower voltage values with increasing wavelength above 760 nm- wavelength. For modern optoelectronic applications, the information about photoelectrical properties of fCNTs in the spectral ranges 800–900 nm and 550–900 nm is important. Mostly, these ranges can be overlapped and correspond to laser lines for different types of solid-state lasers. Also, the laser such as argon, krypton, helium-neon, and ruby with emission wavelengths 490 nm, 630 nm, and 690 nm motivated to investigate the photosensitivity of carbon nanomaterials. Comparisons between the collected data from Figure 1-3 are shown the possibility for their future applications but require the chemical content improvement of carbon nanotubes and new experimental conditions.

5. Conclusions

The dependencies of photosensitivity spectra for the fCNT doped with carboxyl group in the wavelength range from 400 nm to 900 nm under voltage values 1V, 3V, 5V, 7V, and 9V have been investigated. The lowest photosensitivity for the fCNTs at a voltage value equal to 1V was registered. This feature takes place almost along the entire above-mentioned wavelength range and characterizes these materials and voltage value (1V) as unsuitable as a light detector. It is important to note that more effective conditions for fCNTs use in the spectral range of 400-800 nm are voltage 3V and 5V. Moreover, the voltage of 5 V leads to the appearance of the widest and the highest photosensitivity at the wavelength 720 nm with an intensity of 2.67 μA . This makes it important to use it as a light detector in different wavelength ranges.

The I-V experimental data for fCNTs have been shown for different wavelengths of excitation light such as ~640 nm, ~720 nm, ~740 nm, ~760 nm, ~780 nm, and ~880 nm, respectively. The approximated approach has been proposed for describing these experimental curves. The fourth-order polynomials described these experimental data. The approximation has been obtained using MATLAB R2021a software. The I-V characteristics for fCNTs at wavelengths 760 nm and 780 nm have the same shape. But, there is some difference related to the tendency of the photosensitivity peak which shifted towards the lower photocurrent value with the increasing wavelength from 760 nm.

References

- [1] R.G. Abaszade, S.A. Mamedova, F.H. Agayev, S.I. Budzulyak, O.A. Kapush, M.A. Mamedova, A.M. Nabiyeu, *Physics and Chemistry of Solid State*, 22(3), pp. 595-601 (2021); <https://doi.org/10.15330/pcss.22.3.595-601>
- [2] R.G. Abaszade, A.G. Mammadov, I.Y. Bayramov, E.A. Khanmammadova, V.O. Kotsyubynsky, O.A. Kapush, V.M. Boychuk, E.Y. Gur, *Physics and Chemistry of Solid State*, 23(2), pp. 256-260 (2022); <https://doi.org/10.15330/pcss.23.2.256-260>
- [3] R.G. Abaszade, A.G. Mammadov, E.A. Khanmammadova, İ.Y. Bayramov, R.A. Namazov, Kh.M. Popal, S.Z. Melikova, R.C. Qasimov, M.A. Bayramov, N.İ. Babayeva, *Journal of Ovonic Research*, 19(2), pp.259-263 (2023); <https://doi.org/10.15251/JOR.2023.193.259>
- [4] R.G. Abaszade, M.B. Babanli, V.A. Kotsyubynsky, A.G. Mammadov, E. Gür, O.A. Kapush, M.O. Stetsenko, R.I. Zapukhlyak, *Physics and Chemistry of Solid State*, 24(1), pp. 153-158 (2023); <https://doi.org/10.15330/pcss.24.1.153-158>
- [5] S.R. Figarova, E.M. Aliyev, R.G. Abaszade, R.I. Alekberov, V.R. Figarov, *Journal of Nano Research Submitted*, 67, pp. 25-31 (2021); <http://dx.doi.org/10.4028/www.scientific.net/JNanoR.67.25>
- [6] R.G. Abaszade, A.G. Mammadov, V.O. Kotsyubynsky, E.Y. Gür, I.Y. Bayramov, E.A. Khanmammadova, O.A. Kapush, *International Journal on Technical and Physical Problems of Engineering*, Issue 51, 14(2), pp.302-306 (2022); <http://www.ijotpe.com/IJTPE/IJTPE-2022/IJTPE-Issue51-Vol14-No2-Jun2022/37-IJTPE-Issue51-Vol14-No2-Jun2022-pp302-306.pdf>
- [7] O.O. Voitsihovska, R.M. Rudenko, V.Y. Povarchuk, A.A. Abakumov, I.B. Bychko, M.O. Stetsenki, M.P. Rudenko, *Materials Letters*, 236, pp.334-336 (2019); <https://doi.org/10.1016/j.matlet.2018.10.119>
- [8] M. Stetsenko, S.A. Pullano, T. Margitych, L. Maksimenko, A. Hassan, S. Kryvyi, R. Hu, C. Huang, R. Ziniuk, S. Golovynskyi, I. Babichuk, B. Li, J. Qu, A.S. Fiorillo, *Nanomaterials*, 9(11), p.1641 (2019); <https://doi.org/10.3390/nano9111641>
- [9] W. Liu, G. Speranza, *Journal of Carbon Research*, C, 5, p.72 (2019); <https://doi.org/10.3390/c5040072>
- [10] Y. Zhou, Y. Fang, R.P. Ramasamy, *Sensors (Basel)*, 19(2) p.392 (2019); <https://doi.org/10.3390/s19020392>
- [11] M. Assali, N. Kittana, S. Alhaj-Qasem, *Scientific Reports*, 12, p.12062 (2022); <https://doi.org/10.1038/s41598-022-16247-7>

- [12] O.A. Stasyuk, A. J. Stasyuk, A. A. Voityuk, M. Sola, *Journal of Organic Chemistry*, 85(18), pp.11721-11731 (2020); <https://doi.org/10.1021/acs.joc.0c01384>
- [13] L. S. Salah, N.Ouslimani, D.Bousba, I.Huynen, Y.Danlée, H.Aksas, *Journal of Nanomaterials*, 2021, pp.1-31 (2021); <https://doi.org/10.1155/2021/4972770>
- [14] R.G. Abaszade, O.A. Kapush, A.M. Nabiyeu, *Journal of Optoelectronic and Biomedical Materials*, 12(3), pp. 61–65 (2020); https://www.chalcogen.ro/61_AbaszadeRG.pdf
- [15] R.G. Abaszade, O.A. Kapush, S.A. Mamedova, A.M. Nabiyeu, S.Z. Melikova, S.I. Budzulyak, *Physics and Chemistry of Solid State*, 21(3), pp. 404-408 (2020); <https://doi.org/10.15330/pcss.21.3.404-408>
- [16] M. Stetsenko, T. Margitych, S. Kryvyi, L. Maksimenko, A. Hassan, S. Filonenko, B. Li, J. Qu, E. Scheer, S.Snegir, *Nanomaterials*, 10(3), p.512 (2020); <https://doi.org/10.3390/nano10030512>
- [17] Boyao Cui, Yanhui Xing, Jun Han, Weiming Lv, Wenxing Lv, Ting Lei, Yao Zhang, Haixin Ma, Zhongming Zeng, Baoshun Zhang, *Chinese Physics. B*, 30(2), 10p. (2021); <http://dx.doi.org/10.1088/1674-1056/abcf41>
- [18] A. Singh, A. Sharma, A. Ahmed, A.K. Sundramoorthy, H. Furukawa, S. Arya, A. Khosla, *Biosensors*, 11(9), p.336 (2021); <https://doi.org/10.3390/bios11090336>
- [19] J. Wang, J. Han, X. Chen, X. Wang, *Info.Mat*, 33(1), pp.1-21 (2019); <https://doi.org/10.1002/inf2.12004>
- [20] H.Y. Shih, Y.T. Chen, N.H. Huang, C.M. Wei, Y.F. Chen, *J.Appl.Phys.*, 109, p.103523 (2011); <https://doi.org/10.1063/1.3590152>
- [21] K. Hemen, V. Harikrishnan, B.S. Dhanraj, K.P. Vijayamohanan, *Appl.Phys.Lett.*, 102, p.143104 (2013); <https://doi.org/10.1063/1.4800236>
- [22] E. Baek, T. Rim, J. Schutt, C.K. Baek, K. Kim, L. Baraban, G. Cuniberti, *Nano Lett.*, 17, p.6727 (2017); <https://doi.org/10.1021/acs.nanolett.7b02788>
- [23] V.M. Boychuk, R.I. Zapukhlyak, R.G. Abaszade, V.O. Kotsyubynsky, M.A. Hodlevsky, B.I. Rachiy, L.V. Turovska, A.M. Dmytriv S.V. Fedorchenko, *Physics and Chemistry of Solid State*, 23(4), pp. 815-824 (2022); <https://doi.org/10.15330/pcss.23.4.815-824>
- [24] R.G. Abaszade, E.M. Aliyev, M.B. Babanli, V.O. Kotsyubynsky, R.I. Zapukhlyak, A.G. Mammadov, H.F. Budak, A.E. Kasapoglu, E. Gür, T.O. Margitych, M.O. Stetsenko, *Physics and Chemistry of Solid State*, 24(3), pp. 530-535, (2023); <https://doi.org/10.15330/pcss.24.3.530-535>
- [25] R.G. Abaszade, *Journal of Optoelectronic and Biomedical Materials*, 14(3), pp. 107–114 (2022); <https://doi.org/10.15251/JOBM.2022.143.107>
- [26] R.G. Abaszade, M.B. Babanli, V.O. Kotsyubynsky, A.G. Mammadov, E. Gür, O.A. Kapush, M.O. Stetsenko, R.I. Zapukhlyak, *Physics and Chemistry of Solid State*, 24(1), pp. 153-158 (2023); <https://doi.org/10.15330/pcss.24.1.153-158>
- [27] A.G. Mammadov, R.G. Abaszade, V.O. Kotsyubynsky, E.Y. Gür, I.Y. Bayramov, E.A. Khanmammadova, O.A. Kapush, *International Journal on Technical and Physical Problems of Engineering*, Issue 51, 14(3), pp.155-160 (2022); <http://www.ijotpe.com/IJTPE/IJTPE-2022/IJTPE-Issue52-Vol14-No3-Sep2022/21-IJTPE-Issue52-Vol14-No3-Sep2022-pp155-160.pdf>
- [28] A.G. Mammadov, R.G. Abaszade, M.B. Babanli, V.O. Kotsyubynsky, E. Gur, B.D. Soltabayev, T.O. Margitych, M.O. Stetsenko, *International Journal on “Technical and Physical Problems of Engineering”*, 15(3), pp.53-58 (2023); <http://www.ijotpe.com/IJTPE/IJTPE-2023/IJTPE-Issue56-Vol15-No3-Sep2023/7-IJTPE-Issue56-Vol15-No3-Sep2023-pp53-58.pdf>
- [29] N.A. Guliyeva, R.G. Abaszade, E.A. Khanmammadova, E.M. Azizov, *Synthesis and analysis of nanosructured graphene oxide*, *Journal of Optoelectronic and Biomedical Materials*, 15(1), pp. 23 – 30 (2023); https://chalcogen.ro/23_GuliyevaNA.pdf
- [30] R. Moradi, N. Pour Khalili, E. Khanmammadova, R. Abaszade, *Handbook of Functionalized Carbon Nanostructures*. Springer, Cham. pp.1-34 (2024); https://doi.org/10.1007/978-3-031-14955-9_71-1